

## Structural evolution induced in the equilibrium immiscible Cu–V system by ion irradiation

This article has been downloaded from IOPscience. Please scroll down to see the full text article.

2003 J. Phys.: Condens. Matter 15 5543

(<http://iopscience.iop.org/0953-8984/15/32/314>)

View [the table of contents for this issue](#), or go to the [journal homepage](#) for more

Download details:

IP Address: 171.66.16.125

The article was downloaded on 19/05/2010 at 15:01

Please note that [terms and conditions apply](#).

# Structural evolution induced in the equilibrium immiscible Cu–V system by ion irradiation

L Hu and B X Liu<sup>1</sup>

Advanced Materials Laboratory, Department of Material Science and Engineering,  
Tsinghua University, Beijing 100084, China

E-mail: dmslhx@tsinghua.edu.cn

Received 4 April 2003, in final form 23 June 2003

Published 1 August 2003

Online at [stacks.iop.org/JPhysCM/15/5543](http://stacks.iop.org/JPhysCM/15/5543)

## Abstract

In the equilibrium immiscible Cu–V system, interesting structural evolution was observed in the Cu–V multilayers upon 200 keV xenon ion beam mixing at 77 K. In the Cu<sub>30</sub>V<sub>70</sub> sample, a unique amorphous phase was formed. In the Cu<sub>74</sub>V<sub>26</sub> sample, an amorphous phase was partially formed and it transformed, after an over-irradiation dose, into a mixture of fcc and bcc solid solutions. The lattice constants of the fcc and bcc solid solutions were determined to be much larger than those of Cu and V, respectively, and can probably be attributed to a strong repulsive interaction between the Cu and V atoms. The observed structural evolution was discussed in terms of a thermodynamic calculation based on Miedema's theory and in terms of atomic collision triggered by ion irradiation.

## 1. Introduction

Ion beam mixing (IBM) of multilayered films has been proved to be a powerful means for forming various non-equilibrium solid phases. Using a scheme of multilayered films prepared by depositing metals A and B alternately, IBM is able to produce an A<sub>x</sub>B<sub>1-x</sub> alloy with no limitation on composition, as the relative thicknesses of metals A and B can be adjusted to obtain an arbitrary  $x$  from 0 to 1. Until now, various non-equilibrium solid phases have been obtained by IBM in a number of binary metal systems, such as amorphous, metastable crystalline and quasi-crystalline phases, since its effective cooling speed was estimated—based on a thermal spike model—to be as high as  $10^{13-14}$  K s<sup>-1</sup> [1–3]. Nonetheless, a clear physical picture is still lacking due to the complexity of the far-from-equilibrium process involved in the energetic ion–solid interactions.

<sup>1</sup> Author to whom any correspondence should be addressed.

**Table 1.** The relative thicknesses of the individual Cu and V layers of the three alloy compositions.

Composition	Cu <sub>30</sub> V <sub>70</sub>	Cu <sub>49</sub> V <sub>51</sub>	Cu <sub>74</sub> V <sub>26</sub>
Number of bilayers	9	9	9
Cu (nm)	1.3	2.4	3.5
V (nm)	3.2	2.0	1.0

**Table 2.** Structural changes observed in the Cu–V multilayered films upon 200 keV xenon IBM at 77 K.

Dose (Xe <sup>+</sup> cm <sup>-2</sup> )	Cu <sub>30</sub> V <sub>70</sub>	Cu <sub>49</sub> V <sub>51</sub>	Cu <sub>74</sub> V <sub>26</sub>
As-deposited	Cu + V	Cu + V	fcc-I + bcc-I
$3 \times 10^{14}$	Cu + V	Cu + V	Cu + V + fcc-I
$9 \times 10^{14}$	Cu + V	Cu + V	Amor. + fcc-I
$2 \times 10^{15}$	Cu + V	Cu + V + fcc-I + bcc-I	Amor. + fcc-I
$6 \times 10^{15}$	Amor.	Cu + V + fcc-I + bcc-I	fcc-I + bcc-I

In this study, the Cu–V system was selected in order to study the possibility of forming non-equilibrium solid phases by IBM. The Cu–V system is characterized by a positive heat of formation (about +7 kJ mol<sup>-1</sup>) [4] and has always been studied using other non-equilibrium materials preparation methods, such as chill block melt-spinning [5], mechanical alloying [6, 7], etc.

## 2. Experimental procedure

The Cu–V multilayered films were prepared by depositing pure copper and vanadium alternately onto freshly cleaved NaCl single-crystal substrates in an electron-gun evaporation system with a vacuum level of the order of 10<sup>-6</sup> Pa. The deposition rate was controlled at 0.05 nm s<sup>-1</sup>. The total thickness of the films was designed to be about 40 nm, which was required to match the projected range plus projected range straggling of 200 keV xenon ions. Three alloy compositions were chosen for the present study, namely Cu<sub>25</sub>V<sub>75</sub>, Cu<sub>50</sub>V<sub>50</sub> and Cu<sub>75</sub>V<sub>25</sub>. The Cu–V multilayered samples were designed to consist of nine bilayers (or 18 layers in total) and the desired overall compositions were obtained by adjusting the relative thicknesses of the individual Cu and V layers, which are listed in table 1. After deposition, the real compositions of the samples were confirmed to be Cu<sub>30</sub>V<sub>70</sub>, Cu<sub>49</sub>V<sub>51</sub> and Cu<sub>74</sub>V<sub>26</sub>, respectively, by energy-dispersive spectrum (EDS) analysis with a measurement error of about 4%. IBM was conducted at 77 K to various doses, ranging from 1 × 10<sup>14</sup> to 8 × 10<sup>15</sup> Xe<sup>+</sup> cm<sup>-2</sup>. The ion current density was confined to 0.5 μA cm<sup>-2</sup> to avoid overheating effects. For structural characterization, all the Cu–V multilayered films were removed from the NaCl substrates using de-ionized water and placed onto the Cu grids for examination by transmission electron microscopy (TEM) and analysis by selected area diffraction (SAD).

## 3. Results and discussion

### 3.1. Experimental results

The structural changes in the Cu–V multilayered films upon 200 keV xenon IBM at 77 K are summarized in table 2. First we discuss the experimental results for the Cu<sub>30</sub>V<sub>70</sub> multilayered films. In the SAD pattern of the as-deposited Cu<sub>30</sub>V<sub>70</sub> sample (figure 1(a)), sharp diffraction

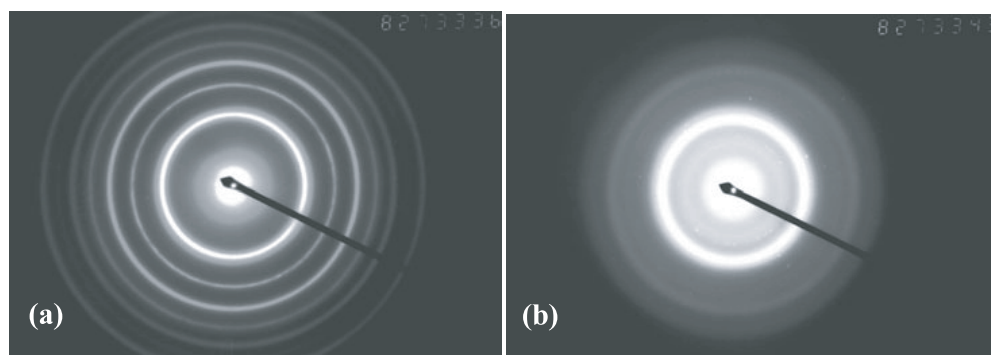
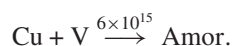
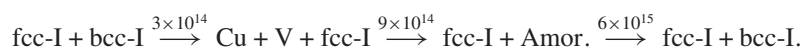


**Figure 1.** (a) An SAD pattern of the as-deposited  $\text{Cu}_{30}\text{V}_{70}$  multilayered films, showing the diffraction lines from polycrystalline Cu(111) and V(110), (200), (211), etc. (b) An SAD pattern taken at an irradiation dose of  $6 \times 10^{15} \text{Xe}^+ \text{cm}^{-2}$ . One can see three haloes, confirming the formation of a unique amorphous Cu–V phase.

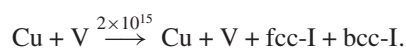
lines reflected from polycrystalline Cu and V can be observed clearly, indicating that, in the as-deposited films, Cu and V were of crystalline structures. After irradiation to a dose of  $6 \times 10^{15} \text{Xe}^+ \text{cm}^{-2}$ , the SAD pattern (figure 1(b)) exhibits three haloes, but no sharp diffraction lines, suggesting that a unique Cu–V amorphous phase has been formed. The structural evolution in the  $\text{Cu}_{30}\text{V}_{70}$  multilayered films upon IBM can therefore be summarized as follows:



For the  $\text{Cu}_{74}\text{V}_{26}$  multilayered films, sharp diffraction lines could also be observed in the SAD pattern of the as-deposited sample (figure 2(a)). However, they were not reflected from the pure Cu and V crystalline metals. Instead, they are reflected from two newly formed phases, which are named fcc-I and bcc-I for convenience. Figures 2(b)–(d) are SAD patterns of the  $\text{Cu}_{74}\text{V}_{26}$  multilayered films upon IBM to doses of  $3 \times 10^{14}$ ,  $9 \times 10^{14}$  and  $6 \times 10^{15} \text{Xe}^+ \text{cm}^{-2}$ , respectively. At the  $3 \times 10^{14} \text{Xe}^+ \text{cm}^{-2}$  irradiation stage, the diffraction lines (figure 2(b)) changed back to those from polycrystalline Cu, V and fcc-I, indicating the disappearance of the bcc-I phase and the appearance of Cu and V metals. At the  $9 \times 10^{14} \text{Xe}^+ \text{cm}^{-2}$  irradiation stage, the diffraction lines from the crystalline Cu and V disappeared again and a halo could be observed clearly together with some weak diffraction lines from the fcc-I phase, suggesting the formation of the Cu–V amorphous phase. When the irradiation dose was raised to  $6 \times 10^{15} \text{Xe}^+ \text{cm}^{-2}$ , only those diffraction lines from the fcc-I and bcc-I phases remained, but no halo could be detected. The structural evolution in  $\text{Cu}_{24}\text{V}_{76}$  can therefore be summarized as follows:



In the  $\text{Cu}_{49}\text{V}_{51}$  multilayered films, the microstructure of the multilayered films in the as-deposited state were crystalline Cu and V. These then changed partially to the fcc-I and bcc-I phases upon IBM at a dose of  $2 \times 10^{15} \text{Xe}^+ \text{cm}^{-2}$ . The structural evolution in the  $\text{Cu}_{49}\text{V}_{51}$  can therefore be summarized as follows:



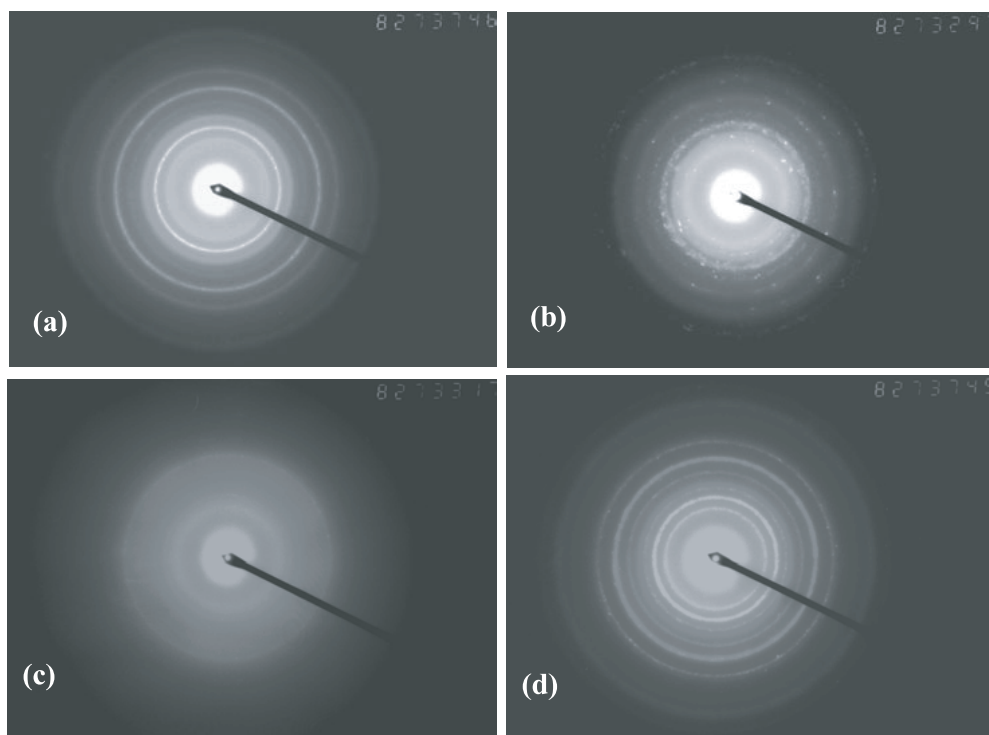


**Figure 2.** (a) An SAD pattern of the as-deposited  $\text{Cu}_{74}\text{V}_{26}$  multilayered films, showing the diffraction lines from polycrystalline fcc-I [(111), (200), etc] and bcc-I [(110), (200), (211), etc]. SAD patterns taken at irradiation doses of  $3 \times 10^{14}$ ,  $9 \times 10^{14}$  and  $6 \times 10^{15} \text{Xe}^+ \text{cm}^{-2}$  are shown in (b), (c) and (d), respectively: (b) polycrystalline Cu, V and fcc-I; (c) polycrystalline fcc-I and amorphous phase; (d) polycrystalline fcc-I and bcc-I.

### 3.2. Identification of the fcc-I and bcc-I phases

In the  $\text{Cu}_{74}\text{V}_{26}$  and  $\text{Cu}_{49}\text{V}_{51}$  samples, fcc-I and bcc-I phases were obtained and considered as the Cu-based and V-based solid solutions, respectively, since the crystal lattices of Cu and V are also fcc and bcc structures, respectively. After consulting the equilibrium phase diagram of the Cu–V system, we found that the solid solutions of V in Cu (<0.1 at.%) and Cu in V (<3 at.%) at room temperature were both very small. We thus deduced that the newly formed fcc-I and bcc-I phases were super-saturated solid solutions, which can be considered as metastable crystalline phases. Through measuring the diffraction lines in the SAD patterns, the lattice parameters of the fcc-I and bcc-I structures, as well as those of Cu and V, were determined. Taking the  $\text{Cu}_{74}\text{V}_{26}$  sample as an example, the lattice parameters of the fcc-I and bcc-I structures were determined to be about 0.42 and 0.43 nm, respectively, which are much larger than the lattice parameters of Cu (0.36 nm) and V (0.3 nm), respectively. Similar results were also obtained for the  $\text{Cu}_{49}\text{V}_{51}$  sample.

As mentioned above, the Cu–V system has positive heat of formation, thus Cu and V atoms are repulsive to each other. Since the observed fcc-I and bcc-I solid solutions are both composed of Cu and V, it can be deduced that the lattice parameters of the two phases should increase due to the strong repulsive interaction between the immiscible Cu and V atoms.

### 3.3. Thermodynamic consideration

We now discuss the mechanism of the structural evolution that is observed in the Cu–V multilayered films upon IBM. Generally, the IBM process can be divided into two steps, i.e. a first step of atomic collision cascade triggered by impinging ions followed by a second step of relaxation [8]. In the first step, many atoms are excited into motion and cannot organize themselves in an ordered atomic configuration. It is therefore recognized that the structure of an alloy phase that is to be formed in IBM can only be fixed during the second step of relaxation. As the energy of the irradiating ions is 200 keV (which is much higher than the typical binding energy of the solids of 5–10 eV), the irradiating ions trigger a series of atomic collisions—namely atomic collision cascade—which is certainly far from equilibrium. While receiving an adequate ion dose, the layered structure of the multilayered films is smeared out, resulting in a uniform mixture of A and B atoms in a highly energetic state. At the moment of termination of the atomic collision cascade, the highly energetic mixture somehow relaxes towards equilibrium. At this very moment, the equilibrium thermodynamics begins to play a role and govern the direction of relaxation as well as indicating the possible intermediate/metastable states in which the atomic mixture reside. In this sense, the free-energy calculation based on equilibrium thermodynamics can be applied to discuss the metastable phase formation during the relaxation period. In this study, Miedema's model [4] and the method proposed by Alonso *et al* [9] were employed to calculate the free energies of the alloy phases in question.

The Gibbs free energy of an alloy phase can be calculated from  $\Delta G = \Delta H - T\Delta S$ , where  $\Delta H$  and  $\Delta S$  are the enthalpy and entropy terms, respectively. As a first approximation, the entropy term for a solid solution and an amorphous phase is taken simply as that of an ideal solid solution, i.e.

$$\Delta S = -R(X_A \ln X_A + X_B \ln X_B)$$

in which  $R$  is the gas constant and  $X_A$  and  $X_B$  are the atomic concentrations of A and B metals, respectively. According to Miedema's model, the change in enthalpy,  $\Delta H$ , can be a sum of three terms [10–12]:

$$\Delta H = \Delta H^C + \Delta H^e + \Delta H^S.$$

In the above equation,  $\Delta H^C$ ,  $\Delta H^e$  and  $\Delta H^S$  refer to the chemical, elastic and structural contributions, respectively.

The chemical contribution  $\Delta H^C$ , which is due to the electron redistribution generated at the surface of contact between dissimilar atomic cells, is expressed by [13]

$$\Delta H^C = X_A f_{AB} \Delta H_{\text{amp}}$$

where  $\Delta H_{\text{amp}}$  refers to an amplitude concerning the magnitude of the electron redistribution interaction.

The elastic contribution,  $\Delta H^e$ , originates from an atomic size mismatch and can be derived from the following equation [14–17]:

$$\Delta H^e = X_A X_B [X_A \Delta H_{(\text{B in A})}^e + X_B \Delta H_{(\text{A in B})}^e].$$

where  $\Delta H_{(i \text{ in } j)}^e$  stands for an elastic contribution to the heat of solution of  $i$  in  $j$  and can be calculated by the elastic constants of the constituent metals [18, 19].

The structural contribution,  $\Delta H^S$ , reflects the correlation between the number of valence ( $s + d$ ) electrons and the crystal structure of the transition metals. The expression for this term reads [18, 19]

$$\Delta H^S = E(Z) - X_A E(Z_A) - X_B E(Z_B).$$

In the equation,  $E(Z)$ ,  $E(Z_A)$  and  $E(Z_B)$  are the lattice stability parameters [10, 12] of the alloy phase and the pure metals of A and B, respectively.  $Z$ ,  $Z_A$  and  $Z_B$  are the average numbers of valence electrons of the alloy phase and the pure metals A and B, respectively. The dependence of the lattice stability on  $Z$  for the paramagnetic transition metals of bcc, fcc and hcp structures has been calculated by Niessen and Miedema [10]. Corrections for the systems including ferromagnetic metals have also been reported by Niessen and Miedema [13].

For the enthalpy of an amorphous phase, both elastic and structural terms are absent. According to Niessen and Miedema, the enthalpy of the amorphous phase is given by [13]

$$\Delta H_{\text{amorphous}} = \Delta H^C + \alpha(X_A T_{m,A} + X_B T_{m,B}).$$

The parameter  $\alpha$  is an empirical constant with a value of  $3.5 \text{ J mol}^{-1} \text{ K}^{-1}$  and  $T_{m,i}$  is the melting point of the component.

For a metastable crystalline (MX) phase, which is considered to be in an ordered structure, its entropy term can be neglected. The free energy of the MX phase includes the following three terms [3]:

$$\Delta G_{\text{MX}} = \Delta H_{\text{MX}}^C + \Delta H_{\text{MX}}^e + \Delta H_{\text{MX}}^S.$$

Besides, the Gibbs free energy of the initial state of the multilayered films consisting of metals A and B can no longer be considered as a ground state of  $G = 0$ , corresponding to a mechanical mixture of crystalline metals A and B in bulk form. Instead, it is a sum of the excess interfacial free energy stored in the multilayered films and that of the ground state ( $G = 0$ ) [3].

The Cu–V system has a positive heat of formation ( $+7 \text{ kJ mol}^{-1}$ ), which is not favourable for the formation of metastable phases, such as the amorphous phase, MX phase, etc. However, in our IBM experiment, through preparing the multilayered films by depositing two metals alternately, the initial energetic state of the multilayered films was elevated by adding the interfacial free energy. As the Cu–V multilayered films consisted of nine bilayers (or 18 layers in total), the free energy of the as-deposited multilayered films is already higher than that of an amorphous phase, so it is possible to form the amorphous phase through IBM.

We first discuss the structural evolution in the  $\text{Cu}_{30}\text{V}_{70}$  multilayered films. Upon IBM at low doses, the sample was still composed of polycrystalline Cu and V. At a sufficient irradiation dose, complete amorphization was indeed achieved, conforming to the calculated results that the free energy of the as-deposited multilayered films ( $30 \text{ kJ mol}^{-1}$ ) was higher than that of an amorphous phase ( $9.4 \text{ kJ mol}^{-1}$ ). In the  $\text{Cu}_{49}\text{V}_{51}$  multilayered films, after irradiation, polycrystalline forms of fcc-I and bcc-I were formed. Their free energies were also much lower than that of the as-deposited multilayered films.

For the  $\text{Cu}_{74}\text{V}_{26}$  multilayered films, the situation was a little more complex. In the as-deposited sample, the fcc-I and bcc-I phases were already formed due to the solid-state reaction taking place during deposition, since the free energy of the as-deposited sample ( $27.2 \text{ kJ mol}^{-1}$ ) was much higher than those of the super-saturated solid solutions. Moreover, during deposition the substrate temperature was higher than room temperature, which enhanced the solid-state reaction. For low-dose irradiation, some of the fcc-I phase and all of the bcc-I phase turned into polycrystalline Cu and V, suggesting that fcc-I and bcc-I were not stable and transformed into some possible states of lower free energy, as indicated in the equilibrium phase diagram. After irradiation to a high dose, the Cu–V amorphous phase appeared in the sample. Since the relaxation step in IBM was very short, a highly energetic mixture of Cu and V atoms was probably unable to organize itself into an ordered atomic configuration, thus leading to the formation of the Cu–V amorphous phase. Besides, the presence of some remaining Xe ions in the Cu–V sample may also help to stabilize the amorphous phase. Further irradiation decomposed the amorphous phase into a mixture of the fcc-I and bcc-I phases again,

suggesting that the free energies of the super-saturated solid solutions were lower than that of the amorphous phase ( $9.1 \text{ kJ mol}^{-1}$ ).

#### 4. Conclusion

- (a) An amorphous alloy could indeed be obtained in the immiscible Cu–V system by 200 keV xenon IBM at 77 K in properly designed Cu–V multilayered films possessing adequate interfacial free energy.
- (b) A series of fcc and bcc super-saturated solid solutions were formed in the  $\text{Cu}_{74}\text{V}_{26}$  and  $\text{Cu}_{49}\text{V}_{51}$  samples. Their lattice parameters were much larger than those of Cu and V, respectively, and are thought to be a natural consequence of a strong repulsive interaction between the immiscible Cu and V atoms.

#### Acknowledgments

The authors are grateful for financial support from the National Natural Science Foundation of China, the Ministry of Science and Technology of China (G20000672), and from Tsinghua University.

#### References

- [1] Liu B X, Johnson W L, Nicolet M-A and Lau S S 1983 *Appl. Phys. Lett.* **42** 45
- [2] Hung L S, Nastasi M, Gyulai J and Mayer J W 1983 *Appl. Phys. Lett.* **42** 672
- [3] Liu B X, Lai W S and Zhang Q 2000 *Mater. Sci. Eng. R* **29** 1
- [4] de Boer F R, Boom R, Matter W C, Miedema A R and Niessen A K 1989 *Cohesion in Metals: Transition Metal Alloys* (Amsterdam: North-Holland)
- [5] Bell A and Davies H A 1997 *Mater. Sci. Eng. A* **226** 1039–41
- [6] Baricco M, Battezzati L, Enzo S, Soletta I and Cocco G 1993 *Spectrochim. Acta A* **49** 1331–44
- [7] Fukunaga T, Mori M, Inou K and Mizutani U 1991 *Mater. Sci. Eng. A* **134** 863–6
- [8] Liu B X and Jin O 1997 *Phys. Status Solidi a* **161** 3
- [9] Alonso J A, Gallego L J and Simozar J A 1990 *Nuovo Cimento* **12** 587
- [10] Niessen A K and Miedema A R 1983 *Ber. Bunsenges. Phys. Chem.* **87** 717
- [11] Lopez J M and Alonso J A 1985 *Z. Naturf. a* **40** 1199
- [12] Weeber A W 1987 *J. Phys. F: Met. Phys.* **17** 809
- [13] Niessen A K, Miedema A R, de Boer F R and Boom R 1988 *Physica B* **152** 303
- [14] Lopez J M and Alonso J A 1983 *Phys. Status Solidi a* **76** 675
- [15] Lopez J M and Alonso J A 1984 *Phys. Status Solidi a* **85** 423
- [16] Friedel J 1954 *Adv. Phys.* **3** 446
- [17] Eshelby J D 1956 *Solid State Phys.* **3** 79
- [18] Lopez J M and Alonso J A 1985 *Z. Naturf. a* **40** 1199
- [19] Loeff P I, Weeber A W and Miedema A R 1988 *J. Less-Common Met.* **140** 299